Available at www.sciencedirect.com

ScienceDirect

journal homepage: www.elsevier.com/locate/watres

Preparation, stabilization and characterization of TiO_2 on thin polyethylene films (LDPE). Photocatalytic applications

Yu Zhiyong[a,f], E. Mielczarski[b], J. Mielczarski[b], D. Laub[c], Ph. Buffat[c], U. Klehm[d], P. Albers[d], K. Lee[e], A. Kulik[e], L. Kiwi-Minsker[a], A. Renken[a], J. Kiwi[a,*]

[a]Institute of Chemical Sciences and Engineering, LGRC, Station 6, EPFL, 1015 Lausanne, Switzerland
[b]INPL/CNRS, UMR 7569 LEM, 15 av du Charmois, 54501 Vandoeuvre les Nancy, France
[c]Interdepartmental Institute of Electron Microscopy (CIME), Station 12, EPFL, 1015 Lausanne, Switzerland
[d]AQura GmbH Industriepark Wolfgang, Rodenbacher Chaussee 4, D-63457 Hanau, Germany
[e]Institute of Physics of Complex Matter, Station 9, EPFL, 1015 Lausanne, Switzerland
[f]Department of Chemistry, Renmin University of China, 100872 Beijing, China

ARTICLE INFO

Article history:
Received 7 July 2006
Received in revised form
1 November 2006
Accepted 14 November 2006

Keywords:
Photodiscoloration
Polyethylene low-density films
Orange II
Electron microscopy
X-ray photoelectron spectroscopy

ABSTRACT

An innovative way to fix preformed nanocrystalline TiO_2 on low-density polyethylene film (LDPE-TiO_2) is presented. The LDPE-TiO_2 film was able to mediate the complete photodiscoloration of Orange II using about seven times less catalyst than a TiO_2 suspension and proceeded with a photonic efficiency of ~0.02. The catalyst shows photostability over long operational periods during the photodiscoloration of the azo dye Orange II. The LDPE-TiO_2 catalyst leads to full dye discoloration under simulated solar light but only to a 30% TOC reduction since long-lived intermediates generated in solution seem to preclude full mineralization of the dye. Physical insight is provided into the mechanism of stabilization of the LDPE-TiO_2 composite during the photocatalytic process by X-ray photoelectron spectroscopy (XPS). The adherence of TiO_2 on LDPE is investigated by electron microscopy (EM) and atomic force microscopy (AFM). The thickness of the TiO_2 film is seen to vary between 1.25 and 1.69 μm for an unused LDPE-TiO_2 film and between 1.31 and 1.50 μm for a sample irradiated 10 h during Orange II discoloration pointing out to a higher compactness of the TiO_2 film after the photocatalysis.

1. Introduction

In the field of environmental chemistry, semiconductor mediated photocatalysis has been the focus of recent attention since it aims at the destruction of contaminants in water under mild conditions. The objective in this field is to find innovative low cost processes that can use sunlight as the source of irradiation (Oppenlaender, 2003; Mills and Lee, 1997). Suspensions of TiO_2 as photocatalysts present two major drawbacks: (a) the separation of TiO_2 after the treatment, and (b) the low quantum efficiency of these processes. Suitable supports for TiO_2 have been reported recently such as: Nafion (Fernandez et al., 1999), Raschig rings (Bozzi et al., 2004), polyethylene-maleic anhydride copolymer (Dhananjeyan et al., 2001) and synthetic fabrics (Bozzi et al., 2005). Suitable thin film supports should present four properties: (a) withstand reactive oxidative radicals attack during light, (b) maintain adequate long-term catalytic stability, (c) preclude TiO_2 leaching during the light irradiation, and (d) allow photocatalytic reaction to proceed with an acceptable kinetics. The photocatalyst presented in this work shows these properties suitable for reuse during long-term reactor operation.

*Corresponding author. Tel.: +41 021 693 3621; fax: +41 021 693 4111.
E-mail address: john.kiwi@epfl.ch (J. Kiwi).
0043-1354/$ - see front matter © 2006 Elsevier Ltd. All rights reserved.
doi:10.1016/j.watres.2006.11.020

The commercial use of polyethylene thin films is due to the single bond presence that makes this material stable towards chemical and/or corrosive agents. This film is a flexible semi-transparent low-cost commercial product. Polyethylene has excellent electrical properties making it widely used as insulator. The low-density polyethylene used consists of highly branched low crystalline units with the formula $H(CH_2CH_2)_nH$.

Few studies have reported the use of TiO_2 on thin polyethylene films as photocatalyst. Recently, TiO_2 films by sol–gel processing (Yu et al., 2000; Sung et al., 2004) and the degradation of organic compounds under light by TiO_2 fixed on foamed polyethylene sheet have been recently reported (Naskar et al., 1998).

This study presents LDPE-TiO_2 films as photocatalysts showing a stable performance during the photoinduced discoloration of Orange II. The photodiscoloration process will be shown to proceed with an acceptable kinetics having the advantage over nanocrystalline suspensions of TiO_2 requiring a much lower TiO_2 concentration per unit volume to photodegrade azo dyes. LDPE-TiO_2 films avoid the screening of the incident light as it is the case of TiO_2 suspensions. Studies involving the abatement of azo-dyes in suspensions of TiO_2 have been previously reported (Morrison et al., 1996).

In this study we report LDPE-TiO_2 thin films as photocatalyst in processes activated by simulated solar irradiation. We will present the details of the TiO_2 loading procedure. The use of XPS spectroscopy will give detailed information on the surface composition and profile of the outermost catalyst layers (at a few nanometers) involved in the dye discoloration process. The detailed dynamics of the photocatalysis leading to Orange II discoloration and the characterization of the catalyst structure are presented by suitable physical techniques.

2. Methods and materials

2.1. Reagents and materials

Reagents like acid and bases, dye material and H_2O_2 were pro-analysis (p.a.) from Fluka AG Buchs, Switzerland and used without further purification. Millipore-Q tri-distilled H_2O was used throughout this study. The photocatalyst TiO_2 Degussa P25 powder was a gift from Degussa AG, Bäar, Switzerland (Degussa, 1997). The LDPE (0.1 mm thickness) was obtained from Longfellow (ET3112019), had a density of 0.92 g/cm^3, an upper working temperature of 90 °C and a flowing point of 185 °C. The LDPE was prepared by Blown Film Extrusion manufacturing (blownfilm@reifenhauser.com, 1999). This process involves extrusion of a plastic through a circular die, followed by a bubble-like expansion allowing the production of flexible and tough polyethylene multi-layer films.

2.2. Catalyst preparation

A 10 g/l TiO_2 Degussa P25 solution was added to 200 ml isopropanol and aged for a day. The polyethylene film was then introduced in this suspension for 10 h and the film was dried afterwards in air at room temperature (23 °C). The dried film was then heated in an oven at 180 °C for 10 h to diffuse or entrain the nanocrystalline TiO_2 into the polyethylene film. Finally the LDPE-TiO_2 was sonicated for 15 min and washed with tri-distilled water four consecutive times to eliminate the loosely bound TiO_2 particles from the film surface. The pieces of LDPE do not deform at 180 °C and no pyrolysis of LDPE was observed. The Ti^{3+} centers were not observed since they would have induced blue color on the LDPE film (Kiwi, 1986).

2.3. Irradiation procedures and analyses of the irradiated solutions

The photodegradation of Orange II was carried out in small batch cylindrical photochemical reactors made from Pyrex glass (cutoff $\lambda = 290$ nm) of 70 ml capacity containing 50 ml aqueous solution. The strips 48 cm^2 films of LDPE-TiO_2 were positioned immediately behind the reactor wall. Irradiation of the samples was carried out in the cavity of a Suntest solar simulator (Hanau, Germany) air cooled at 35 °C. The light intensity in the cavity of the Suntest simulator at tuned at 100 mW/cm^2 (AM 1) was 2×10^{16} photons/sxcm^2. The Suntest Xe-lamp emitted 7% of the photons in the 290–400 spectral range. The integral radiant flux in the reactor cavity was monitored with a power-meter from YSI Corp. Colorado, USA. The absorption of the solutions was followed in a Hewlett-Packard 38620 N-diode array spectrophotometer. The disappearance of Orange II was measured in the spectrophotometer at $\lambda = 486$ nm (the absorption peak). The peroxide concentrations in the solutions were measured using Merckoquant® paper (Cat Merck No 1.10011.01) for the quantitative detection of peroxides. This is a colorimetric test in which the peroxidase transfers oxygen from the peroxide to the organic redox indicator (o-toluidine) converting it in a blue colored oxidation product. The intensity of the blue color is a function of the peroxide found in solution. This was also carried out for reactions with initially added H_2O_2 to determine its concentration in the course of the reaction.

2.4. Transmission electron microscopy (TEM) and scanning electron microscopy (SEM)

A field emission TEM microscope Philips EM 430 (300 kV) was used to measure the particle size of the nanocrystalline TiO_2 nanocrystalline aggregates on the LDPE surface. Energy dispersive X-ray spectroscopy (EDS) was used to identify the deposition of TiO_2 on the LDPE film. The LDPE film was coated with EPON 812 epoxy resin polymerized at 60 °C and then cut with a microtome at room temperature to a thin layer of ~50 nm thickness. Magnification of 10 000 up to 450 000 × were used to characterize the samples. The resolution normally used was of 0.5 nm.

2.5. Atomic force microscopy (AFM)

The AFM images were acquired in contact mode using a PSIA Xe-100 AFM. The AFM uses a sample driven x–y scanner that is independent from the probe-drive z-scanner, eliminating the background curvature inherent to tube AFM scanners.

Silicon nitride cantilevers were used with feedback set points around 1.0 nN. The images originate from the z-scanner and are not influenced by the non-linearity and the hysteresis of the z-scanner. The AFM scanner and position sensors were calibrated using standard samples from Mikromash. The roughness values involve experimental error below 10%.

2.6. *Elemental analysis*

Elemental analysis of the TiO_2 coverage on LDPE was carried out by atomic absorption spectrometry using a Perkin-Elmer 300S unit.

2.7. *X-ray photoelectron spectroscopy (XPS)*

The XPS was performed using MgK_α radiation of 150 W. The electron energy analyzer (Leybold EA200) was operated with a band pass energy of 75 eV in the pre-selected transmission mode. The binding energy of the spectrometer was referenced to 84.0 eV for the Au $4f_{7/2}$ signal according to the SCA A83 standard of the National Physics Laboratory (Briggs and Shea, 1990). The evaluation of the binding energies of the embedded TiO_2 was carried out following the standard procedures. A reproducibility of $\pm 5\%$ was attained in the XPS measurements. The ADS100 set was utilized to evaluate the XPS data by subtraction of X-ray satellites applying the background correction according to Shirley (1972). The presence of electrostatic charging effects was controlled by measurements including charge compensation by changing the electrostatic potential at the aperture site of the electron energy analyzer.

3. Results and discussions

3.1. *Photodiscoloration of Orange II by LDPE-TiO_2*

Fig. 1 shows the effect on Orange II discoloration by TiO_2 suspensions in the dark (trace a) and under light (trace b). From Fig. 1 (trace a) it is seen that Orange II adsorbs on TiO_2. In the presence of LDPE-TiO_2 film no discoloration was observed in the dark (trace c), but photodiscoloration readily proceeds as shown in trace d. The discoloration of Orange II in Fig. 1 is shown in suspensions (trace a and b) and in thin films (traces c and d). The adsorption of Orange II on TiO_2 became lower when the TiO_2 particle was deposited on the LDPE film. It was stated above that 12.9 mg TiO_2 coated the LDPE film (48.8 cm^2) as compared to 80 mg of TiO_2 in the same 50 ml volume reactor. Therefore, there is a decrease in surface area available for Orange II adsorption and this explains the difference observed in Fig. 1, trace c and Fig. 1, trace a.

The photonic efficiency as defined in Eq. (1) below in the photoreactor is:

$$\text{Photonic efficiency (PE)} = \text{dye molecules reacted/light quanta reaching the reactor wall.} \quad (1)$$

In Fig. 1, traces b it is possible to estimate the PE taking the Suntest light flux as 1.6×10^{16} photons/secxcm^2, the volume in the reactor as ~50 ml and the cell wall surface of 48.8 cm^2, the complete photodiscoloration of Orange II (0.05 mM) within

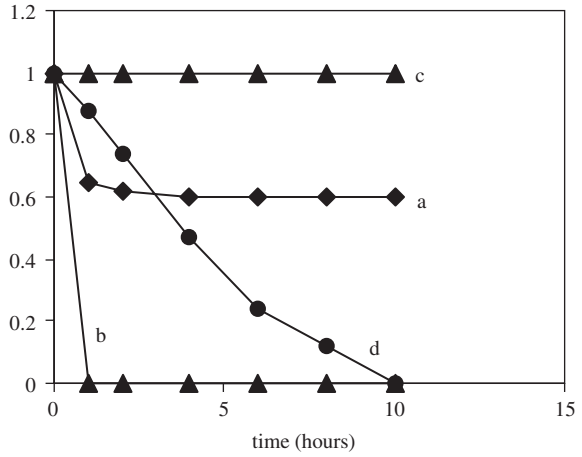

Fig. 1 – Discoloration and discoloration of Orange II (0.05 mM), pH 5.9: (a) dark reaction, TiO_2 Degussa P-25 (1.6 g/L), (b) light reaction with simulated solar light (100 mW/cm^2), TiO_2 Degussa P-25 (1.6 g/L), (c) dark reaction, LDPE-TiO_2 film and (d) light reaction, LDPE-TiO_2 film, with simulated solar light (100 mW/cm^2).

10 h would proceed with a photonic efficiency of ~0.2. By elemental analysis it was found that an LDPE-TiO_2 film under light having 12.9 mg TiO_2 on 48.8 cm^2 was able to fully discolor Orange II in 10 min and that a suspension with 80 mg of TiO_2 in the same 50 ml volume reactor could perform this discoloration within 2 min. Therefore, an LPDE-TiO_2 film on a milligram TiO_2 basis is about six times more effective in Orange II photodiscoloration compared to suspension of TiO_2 (Fig. 1, trace b).

Fig. 2 (trace a) shows that at the initial pH value of 5.9 about 18% photodiscoloration takes place (trace a) and the photodiscoloration is negligible at pH 10 (trace b). Fig. 2 (trace c) shows the favorable effect under light irradiation of the LDPE-TiO_2 film photocatalyst at pH 5.9. When the pH was set to 10 the initial photodiscoloration kinetics becomes slower (trace d). The pH 10 was selected since Orange II has two pK_a values. The first pK_{a1} is at 1.1 and the second pK_{a2} at 11.0 (Bandara and Kiwi, 1999). At pH 10, Orange II shows one negative charge as seen from its formula.

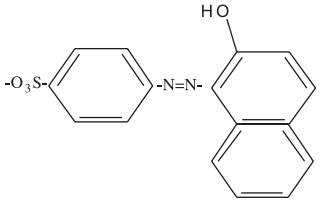

At pH 10, the Orange II is negatively charged and should electrostatically repulse the TiO_2 Degussa P25 that has a negative charge at pH >7.0. The isoelectric point (IEP) of TiO_2 Degussa P25 is 7.0. The initial pH of 10 was set adding NaOH 0.1 M and varied very little during the reaction since TiO_2 has a very well known buffer effect. The more favorable discoloration of Orange II shown in Fig. 2 (trace c) is explained by the sulfonic group attached to Na^+ in Orange II being ionized within the pH range 1.1–7.0 ($pK_{a1} = 1.1$). The negatively Orange II in this region would then interact attractively with

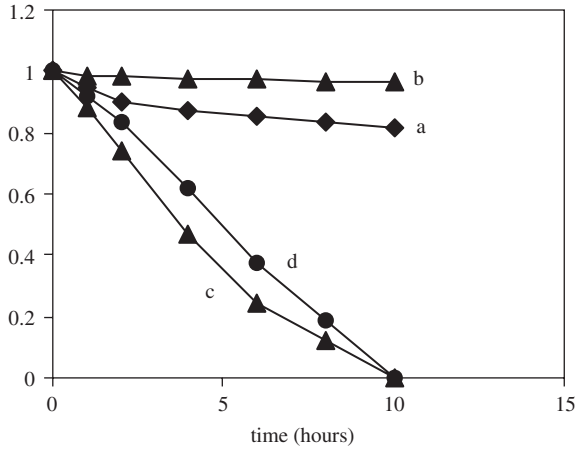

Fig. 2 – Effect of pH on the discoloration of Orange II (0.05 mM) with Suntest solar simulator (100 mW/cm^2): (a) initial pH = 5.9, (b) initial pH = 10.0, (c) LDPE- TiO_2, initial pH = 5.9, and (d) LDPE- TiO_2, initial pH = 10.0.

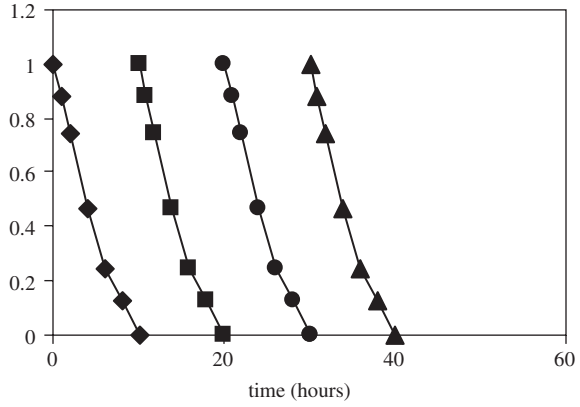

Fig. 3 – Repetitive catalytic photodiscoloration cycles of Orange II (0.05 mM), pH 5.9 with Suntest solar simulator light (100 mW/cm^2) in the presence of LDPE-TiO_2 film.

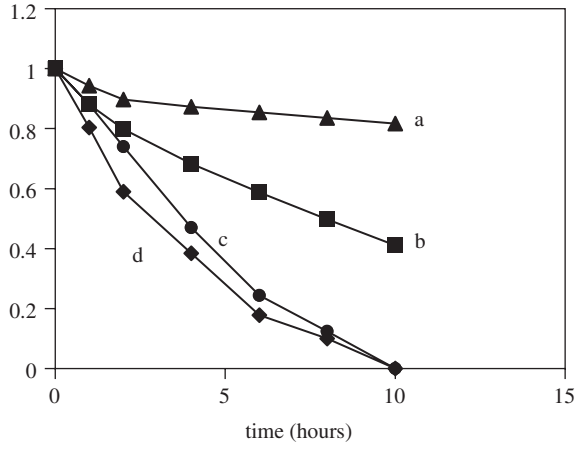

Fig. 4 – Effect of H_2O_2 on the photodiscoloration of Orange II (0.05 mM) with Suntest solar simulated light (100 mW/cm^2) at initial pH = 5.9: (a) Orange II, (b) Orange II, H_2O_2 (10 mM), (c) Orange II in the presence of LDPE-TiO_2 film and (d) Orange II in the presence of LDPE-TiO_2 and H_2O_2 (10 mM).

TiO_2 Degussa P25 charged positively since at pH 5.9 we are below the IEP of TiO_2 Degussa P25.

Fig. 3 shows the stable nature of the LDPE-TiO_2 photocatalyst during repetitive photodiscoloration runs of Orange II. The photodiscoloration runs have been carried out with the same initial concentration of Orange II added in each run. The results shown in Fig. 3 show the capacity of the photocatalyst for its reuse during long-term operation.

The mechanism of azo dye degradation mediated by TiO_2 under light irradiation in the presence of O_2 has been reported and will not be dealt here (Vinodgopal and Kamat, 1994; Bandara and Kiwi, 1999). The dye molecules are excited by the light photons and produce the azo-dye singlet excited state as reported for azo dyes

$$(\text{Orange II})_{ads} + h\nu \rightarrow {}^1(\text{Orange II})^*_{ads}. \quad (2)$$

An electron is injected from the excited state of the adsorbed Orange II in the conduction band of TiO_2 leading to the Orange II cation that subsequently decays:

$${}^1(\text{Orange II})^*_{ads} + TiO_2 \rightarrow {}^1(\text{Orange II})^+_{ads} + TiO_2(e^-_{cb}), \quad (3)$$

and the e^-_{cb} is subsequently scavenged by the O_2 adsorbed on the TiO_2 surface generating the superoxide radical $O_2^{\cdot-}$

$$TiO_2(e^-) + O_2 \rightarrow TiO_2 + O_2^{\cdot-}. \quad (4)$$

The formation of the H_2O_2 (or other oxidative species) active in the photodiscoloration reported in Figs. 1–3 has been reported exhaustively (Mills and Lee, 1997; Kiwi and Grätzel, 1987) and will not be discussed further in this study. The concentrations of H_2O_2 found in solution were observed to remain a relatively low level of ~0.5 mg/L. This value was obtained by using the Merkoquant paper® to detect H_2O_2 formed in solution. The peroxide detection is based on the titration of the o-toluidine on the paper strip turning from white to blue in the presence of peroxides. The detection of H_2O_2 was carried out in air atmosphere and the O_2 in the air present seems to be sufficient to allow reaction (4) to proceed. A fraction of the H_2O_2 produced during the photocatalysis is adsorbed on the TiO_2 surface as reported elsewhere (Kiwi and Grätzel, 1987).

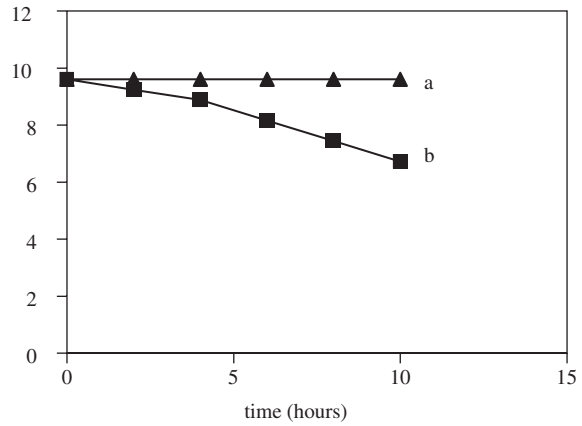

Fig. 5 – TOC decrease of Orange II (0.05 mM) at pH 5.9 in the presence of LDPE-TiO_2 film: (a) dark reaction and (b) reaction under Suntest simulated light (100 mW/cm^2).

Fig. 4 shows the effect of the addition of H_2O_2 in homogeneous solution accelerating the photodiscoloration of Orange II in trace b compared to trace a under light irradiation. In the presence of LDPE-TiO_2 the initial photodiscoloration kinetics is seen to be only slightly enhanced by the addition of H_2O_2 as shown by traces c and d.

The adsorption of O_2 on TiO_2 has been reported to occur only under light irradiation (Oppenlaender, 2003; Mills and Lee, 1997). The results shown in Fig. 4 seem to suggest that the photoadsorption of TiO_2 is the predominant process for LDPE-TiO_2 mediated catalysis leading to the photodiscoloration of Orange II in Fig. 4 since similar discoloration rates were observed on these films in the absence or in the presence of H_2O_2. This is the reason for the modest enhancement observed for the photodiscoloration in trace d with respect to trace c.

Fig. 5 presents the reduction in total organic carbon (TOC) of an Orange II solution (0.05 mM) in the presence of LDPE-TiO_2 film. It is readily seen from Fig. 5 that no TOC reduction is observed in the dark. But under light irradiation about 30% of the initial TOC mineralization was observed. Long-lived intermediates generated in solution precluded further degradation of the dye. We have recently reported the intermediates products of Orange II degradation in two studies (Bandara et al., 1999; Morrison et al., 1996). The Orange II photodiscoloration intermediates within 10 min reaction were identified as oxalic acid, 4-hydroxybenzenosulfonic acid and acetic acid. After 10 min reaction,

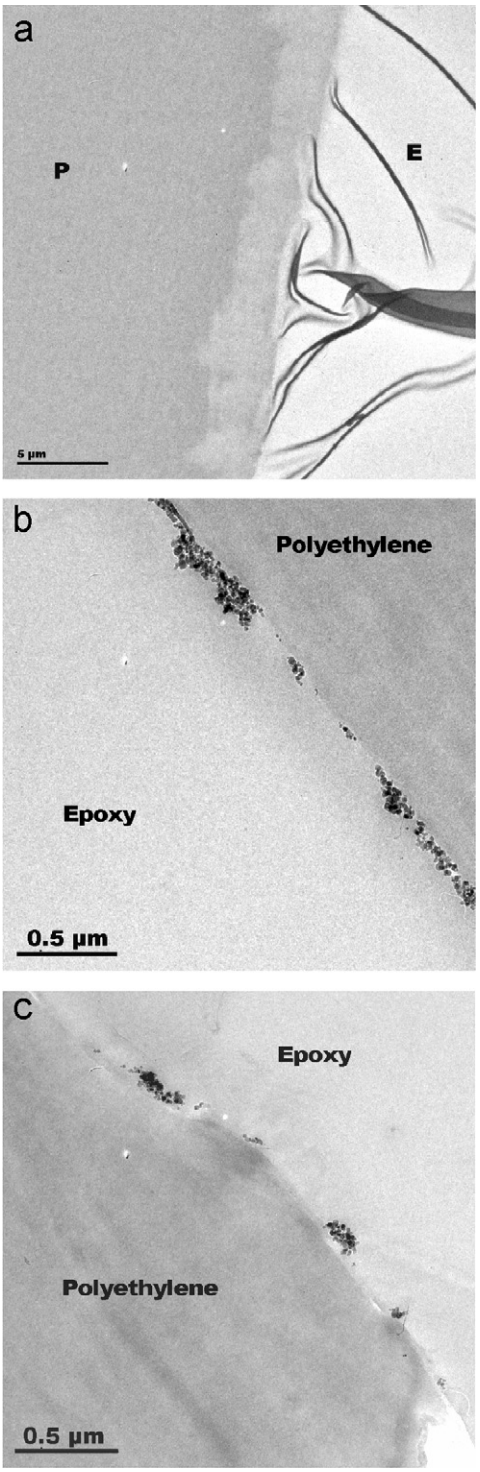

Fig. 6 – (a) Transmission electron microscopy of LDPE film slice of 50 nm enrobed with epoxide. (b) Transmission electron microscopy of LDPE film showing the nanocrystalline TiO_2 (Side 1). (c) Transmission electron microscopy of LDPE film showing the nanocrystalline TiO_2 (Side 2).

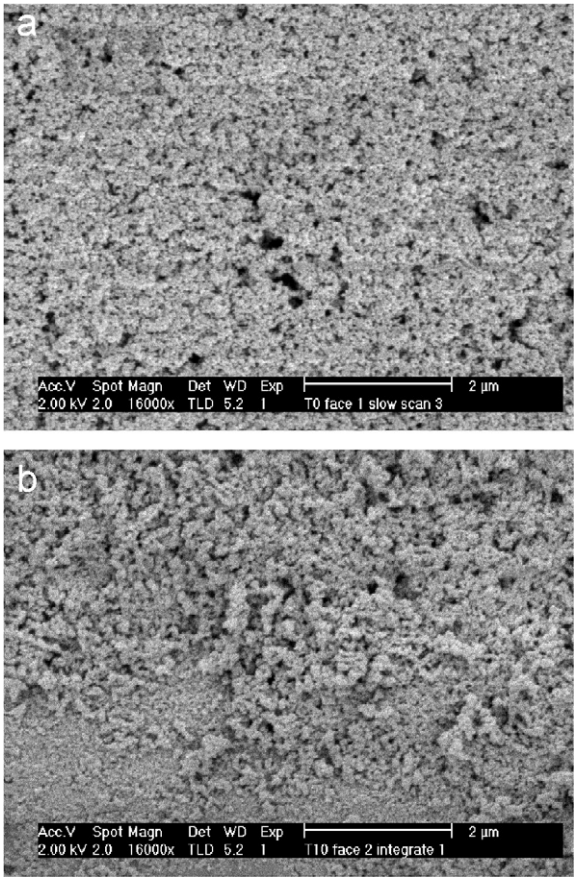

Fig. 7 – (a) Scanning electron microscopy of LDPE film showing the nanocrystalline TiO_2 (Side 1). (b) Scanning electron microscopy of LDPE film showing the nanocrystalline TiO_2 (Side 2).

small amounts of formic and glyoxalic acid were also observed.

3.2. *Transmission electron microscopy (TEM) and scanning electron microscopy (SEM)*

Fig. 6a shows the sample of polyethylene treated in isopropanol and heated for 10 h at 180 °C. Between the polyethylene (P) and the epoxide (E) a clear layer is seen having a low contrast. This makes it impossible to detect the exact nature of this layer. What can be said is that the isopropanol (in air atmosphere) leads to the insertion of some –O– groups on the polyethylene surface during the preparation of the photocatalyst. During the enrobing with epoxide and the cutting of the 50 nm LDPE sample slice, the different elasticity of the epoxide and the polyethylene involved the expansion

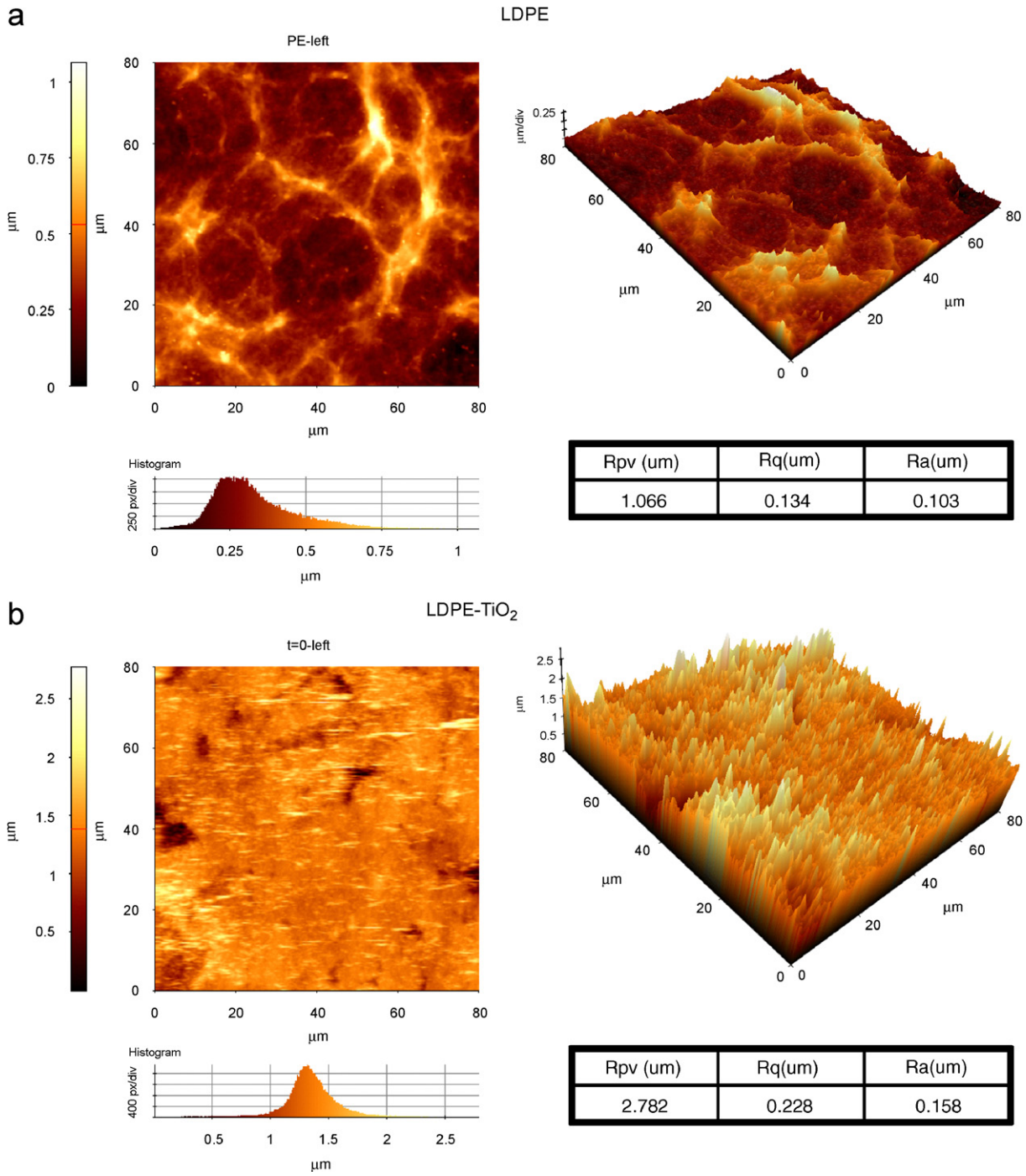

Rpv (um)	Rq(um)	Ra(um)
1.066	0.134	0.103

Rpv (um)	Rq(um)	Ra(um)
2.782	0.228	0.158

Fig. 8 – (a) Atomic force microscopy of the rough side of polyethylene film (LDPE). (b) Atomic force microscopy (AFM) of the rough side of LDPE-TiO_2 at t = 0. (c) Atomic force microscopy (AFM) of the rough side of LDPE-TiO_2 after t = 10 h photocatalysis. (d) AFM of an LDPE-TiO_2 film (time zero) showing the thickness of the TiO_2 layer. (e) AFM of an LDPE-TiO_2 film after 10 h showing the thickness of the TiO_2 layer.

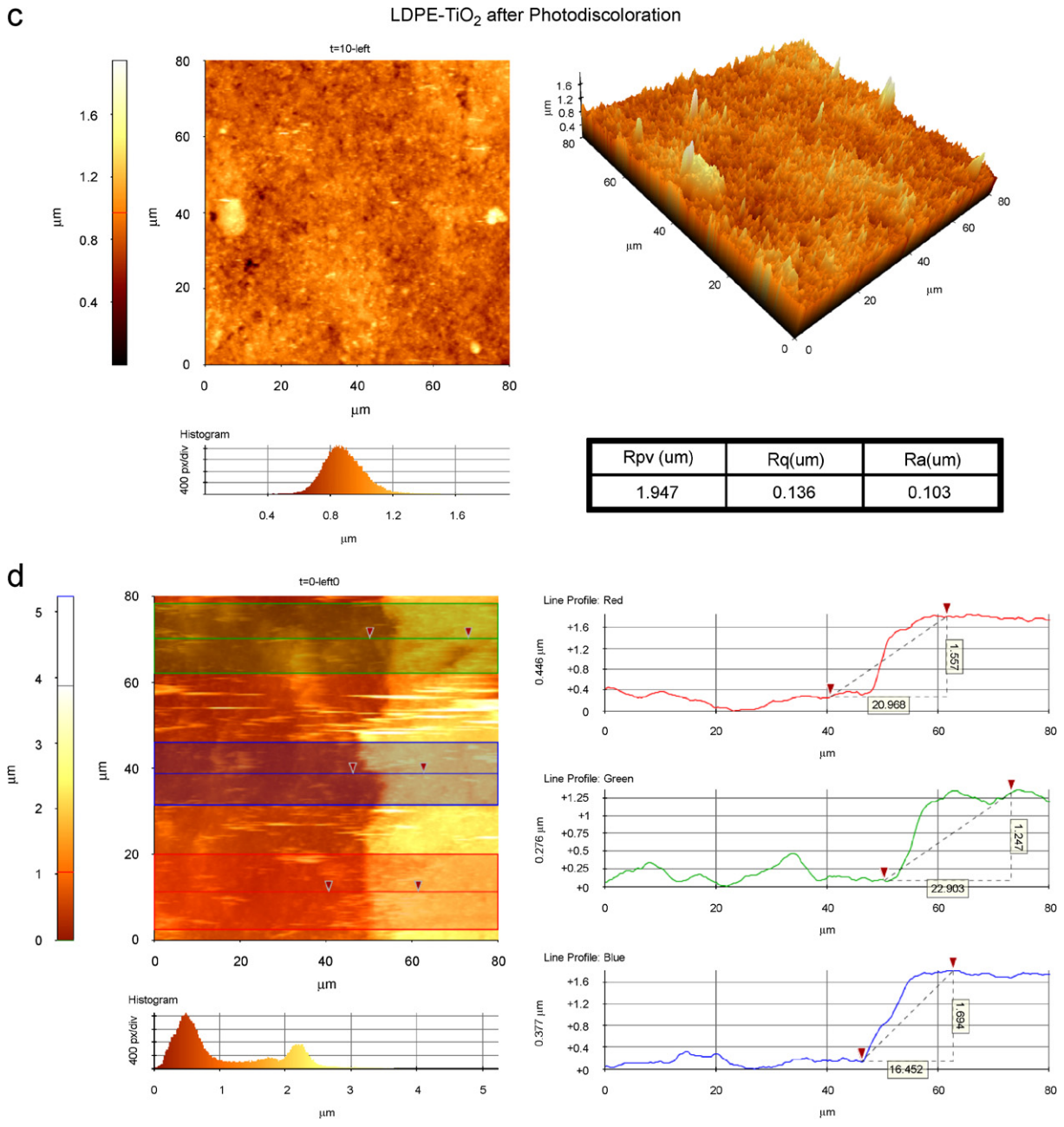

Fig. 8 – (*Continued*)

and retraction of the sample led to pleats (wrinkles) in the epoxide (E) observed in the right hand side in Fig. 6a. Fig. 6b shows the TiO_2 nanocrystals on the side 1 of the polyethylene surface. The TiO_2 layer is not continuous and covers partially the LDPE surface with a variable thickness between 60 and 180 nm.

During the bubble-like expansion step in the manufacturing of LDPE at the bottom of the roller squeeze warmer air inflates the thinner gage. While passing up the tower the roller stretches the outside of the roller (in contact with air) more than the inner side due to the hot air inside the tube and side 1 of LDPE has a higher rugosity than the inner side of the LPDE film with a flatter LDPE surface (side 2) in contact with the glass-wall. This is reflected in the lower value found for the rugosity (Rq) for the side 2 of 0.113 µm. Fig. 6c (side 2) shows a much lower coverage of nanocrystalline TiO_2 on the LDPE film. Side 2 with a lower rugosity allows only for a lower retention of TiO_2. Before and after the photodiscoloration of Orange II the TEM images of the LDPE-TiO_2 did not vary. This is a further proof for the stability of the catalyst as shown previously in Fig. 3.

The scanning electron microscopy of an LDPE-TiO_2 sample (side 1) in Fig. 7a provides the view of a rather homogeneous distribution of TiO_2 with only very few LDPE film areas not covered by TiO_2 as shown by the black holes. Fig. 7b shows an LDPE-TiO_2 sample (side 2) with large areas not covered with TiO_2 in the lower half of Fig. 7b. This is in line with the results obtained by TEM in Fig. 6b for the TiO_2 coverage of LDPE (side 2). Electron energy loss spectrometry (EELS) studies of this

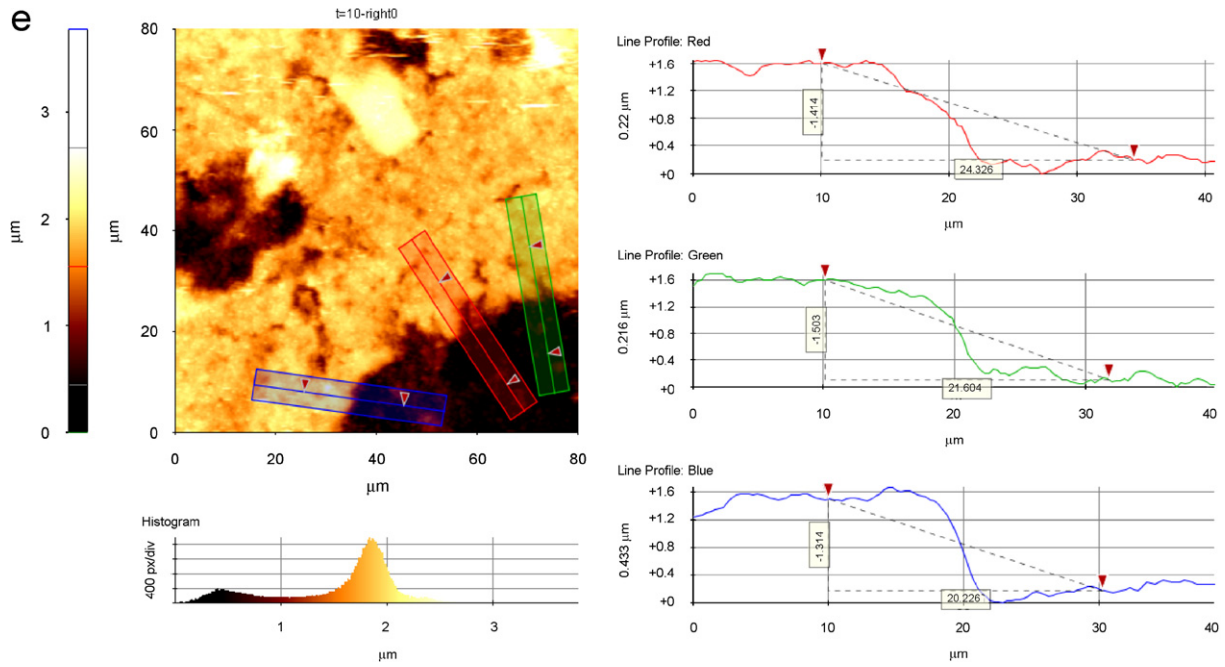

Fig. 8 – (*Continued*)

Table 1 – LDPE and LDPE/TiO_2 XPS peak positions as a function of irradiated time

Peak	Position BE (eV)	FWHM (eV)	Raw area (CPS)	RSF	Atomic mass	Atomic conc (%)	Mass conc (%)
Polyethylene film							
Na 1s	1068.00	2.361	4033.4	1.685	22.990	3.57	5.98
F 1s	683.15	3.480	4203.4	1.000	18.998	7.58	10.50
O 1s	530.60	3.756	4812.8	0.780	15.999	11.48	13.39
N 1s	397.00	4.339	329.5	0.477	14.007	1.32	1.35
Ca 2p	346.90	2.738	405.9	1.833	40.076	0.43	1.25
C 1s	284.60	2.001	10590.1	0.278	12.011	74.58	65.31
Cl 2p	198.50	3.438	49.1	0.891	35.460	0.11	0.29
Si 2p	101.60	3.537	141.5	0.328	28.086	0.95	1.94
LDPE-TiO_2; time zero							
F 1s	686.20	1.681	1573.2	1.000	18.998	3.27	3.27
O 1s	529.45	1.216	14833.0	0.780	15.999	40.80	34.32
Ti 2p	458.25	1.040	13132.5	2.001	47.878	14.25	35.87
N 1s	399.15	1.739	475.4	0.477	14.007	2.19	1.61
C 1s	284.60	1.625	4862.1	0.278	12.011	39.49	24.93
LDPE-TiO_2; time 4 h							
Zn 2p	1021.15	2.633	703.3	5.589	65.387	0.23	0.77
F 1s	686.25	1.899	3967.9	1.000	18.998	8.18	8.09
O 1s	529.25	1.489	13157.1	0.780	15.999	35.92	29.88
Ti 2p	457.95	1.307	12874.9	2.001	47.878	13.87	34.53
N 1s	399.15	2.444	540.9	0.477	14.007	2.48	1.80
Ca 2p	346.55	1.617	209.5	1.833	40.076	0.25	0.53
C 1s	284.60	2.135	4847.8	0.278	12.011	39.08	24.41
LDPE-TiO_2; time 10 h							
F 1s	683.25	1.947	1141.0	1.000	18.998	2.52	2.29
O 1s	529.10	1.250	16140.6	0.780	15.999	47.23	36.06
Ti 2p	457.80	1.079	16411.5	2.001	47.878	18.95	43.29
N 1s	398.80	1.742	921.5	0.477	14.007	4.52	3.02
C 1s	284.60	1.935	3098.2	0.278	12.011	26.77	15.34

sample provided evidence for Ti^{4+} and Ti^{+3} in the TiO_2 as a non-stoichiometric TiO_x ($4>x>3$). It was not possible to quantify further the stoichiometry of the TiO_2 oxide(s).

3.3. *Atomic force microscopy (AFM) studies*

Fig. 8a presents the AFM of the LDPE rougher side (Face 1) showing an rms roughness or rugosity (Rq) of 0.134 μm, an average roughness (Ra) of 0.103 μm and a peak height (distance from the peak to the bottom of the valley) Rpv of 1.066 μm. The histogram of the peak height values is also shown in the lower left-hand side of Fig. 8a. Long crevices are observed in the 2D of the AFM projection of 80×80 μm. The dark sections refer to the crevices (valleys) while the clear sections refer to the peak heights.

Fig. 8b shows the AFM of an LDPE-TiO_2 sample (side 1) with an Rq value of 0.228 μm. The TiO_2 layer does not cover the whole LDPE surface and the Rpv is seen to increase to 2.782 μm due to the TiO_2 present. The spikes on the 3D image in Fig. 8b come from some glitches in the AFM image. These glitches are probably caused by small TiO_2 nanocrystals on LDPE surface that are not fixed in a stable way. The peak height is the distance between the peak of the TiO_2 layer and the bottom of the LDPE film and is bigger than the thickness of the TiO_2 layer on LDPE (side 1) in Fig. 6b. Face 1 seems to provide the most favorable roughness (rms) to attach the Degussa TiO_2 P25 having 20–30 nm nanocrystals to LDPE. This rms value is higher than the one available in face 2 and leads to an improved TiO_2 nanocrystal retention. The TiO_2 retention on LDPE depends on the size and shape of the nanocrystalline TiO_2 resulting in the entrapment and protection of TiO_2 in the 3D LDPE matrix. The histogram reveals a peak height distribution between 1.0 and 2.0 μm.

Fig. 8c shows the LDPE-TiO_2 film after 10 h photodiscoloration of Orange II. It is readily seen that the TiO_2 layer becomes more densely packed compared to the TiO_2 layer reported in Fig. 8b. The TiO_2 layer becomes more uniform and this is reflected in the value of the rugosity Rq of 0.136 μm. The histogram of the rugosity in the lower left-hand side of Fig. 8c show values between 0.6 and 1.2 which are smaller than the corresponding values at time zero (Fig. 8b). The long crevices have disappeared in Fig. 8c compared to Fig. 8b and rather small well-distributed pores remain as seen in the corresponding 2D images.

Fig. 8d, shows in the left-hand side the LDPE-TiO_2 film thickness at time zero (before the Orange II photodiscoloration process). The darker base section corresponds to the thickness of the LDPE film and the clear section to the right-hand side to the TiO_2 deposit in the 80×80 μm square of the sample taken for analysis. From the three line profiles shown on the right-hand side in Fig. 8d, the thickness of the TiO_2 film is seen to vary between 1.25 and 1.69 μm (see vertical numbers in the profile plot).

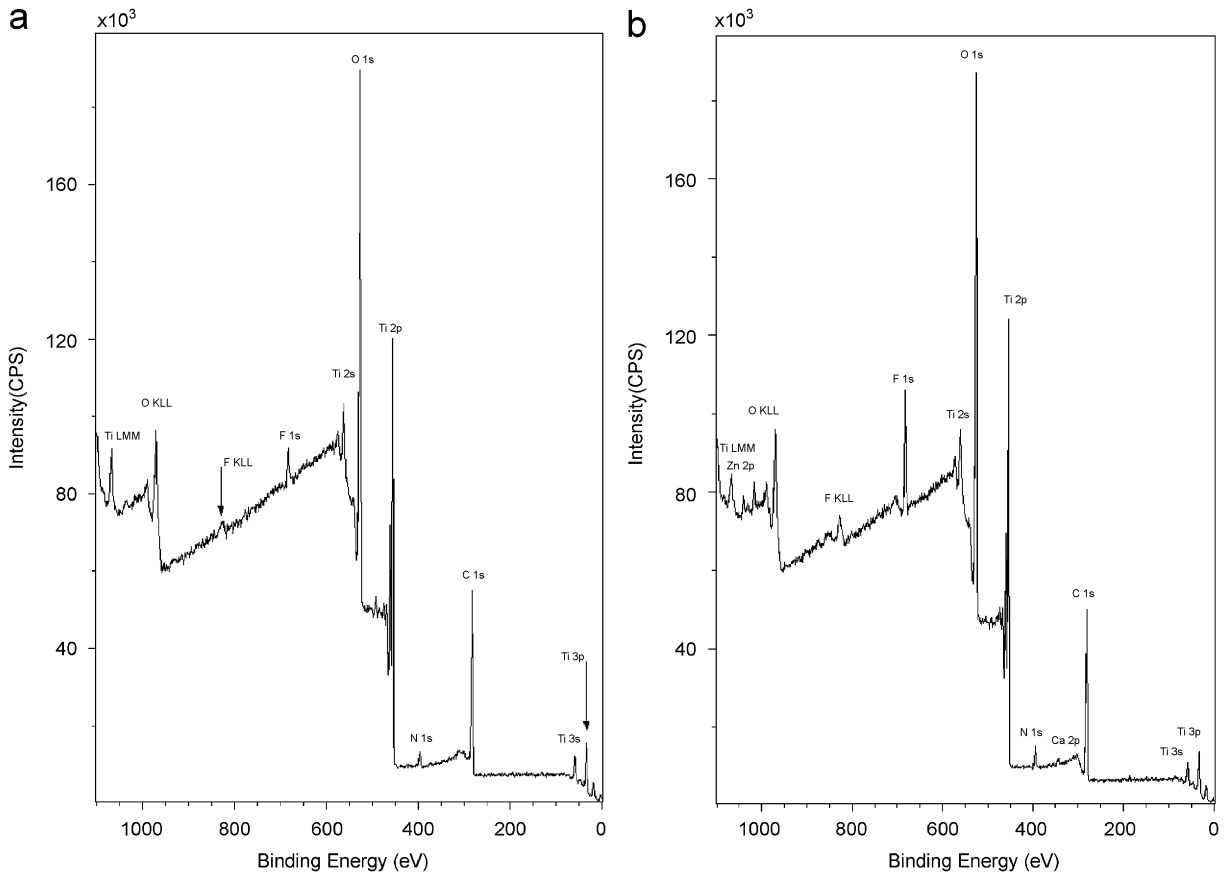

Fig. 9 – (a) XPS of the LDPE-TiO_2 surface at $t = 0$; (b) XPS of the LDPE-TiO_2 surface at $t = 4$ h; (c) XPS of the LDPE-TiO_2 surface at $t = 10$ h.

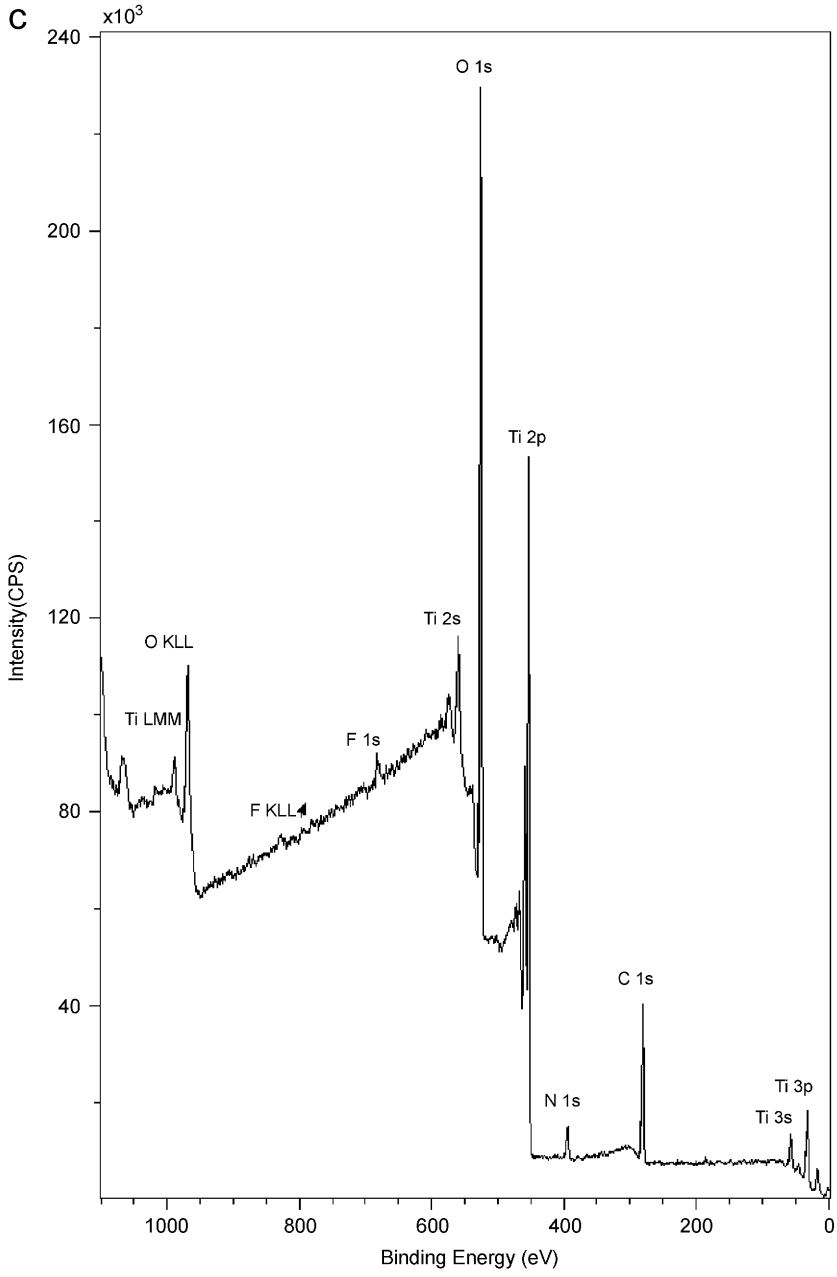

Fig. 9 – (*Continued*)

Fig. 8e shows the same data for the LDPE-TiO_2 film thickness after 10 h photodiscoloration of Orange II. From the three line profiles shown on the right-hand side in Fig. 8e, the thickness of the TiO_2 film is seen to vary between 1.31 and 1.50 μm (see vertical numbers in the profile plot). The higher compactness of the TiO_2 film after the photocatalysis is in agreement with the results reported above when comparing the observations reported in Fig. 8c with respect to Fig. 8b.

3.4. *X-ray photoelectron spectroscopy (XPS) of LDPE-TiO_2 films*

The XPS spectroscopy allows the determination of the surface composition of the 2 nm topmost layers with very high surface sensitivity for LDPE and the LDPE-TiO_2 films as shown in Table 1. LDPE showed the atomic surface concentration percentages for the following major elements: O(11.46%), C(74.58%). Elements like Na, Ca, N, and Si are present in the LDPE surface are introduced in the LDPE film during the manufacturing process (see Table 1). These elements were washed out during the LDPE-TiO_2 catalyst preparation. LDPE shows the major component C1 s lines at 284.6 eV of the CH-group. There is also the O1 s line at 529.1 eV indicating the presence of surface OH-groups. These groups are always present when TiO_2 is exposed to air.

Fig. 9a shows the XPS spectra of LDPE-TiO_2 at time zero in the topmost atomic layers. The C-concentration represented by the $(–CH_2)_n$ peak at 284.6 eV (Wagner et al., 1989) is seen to

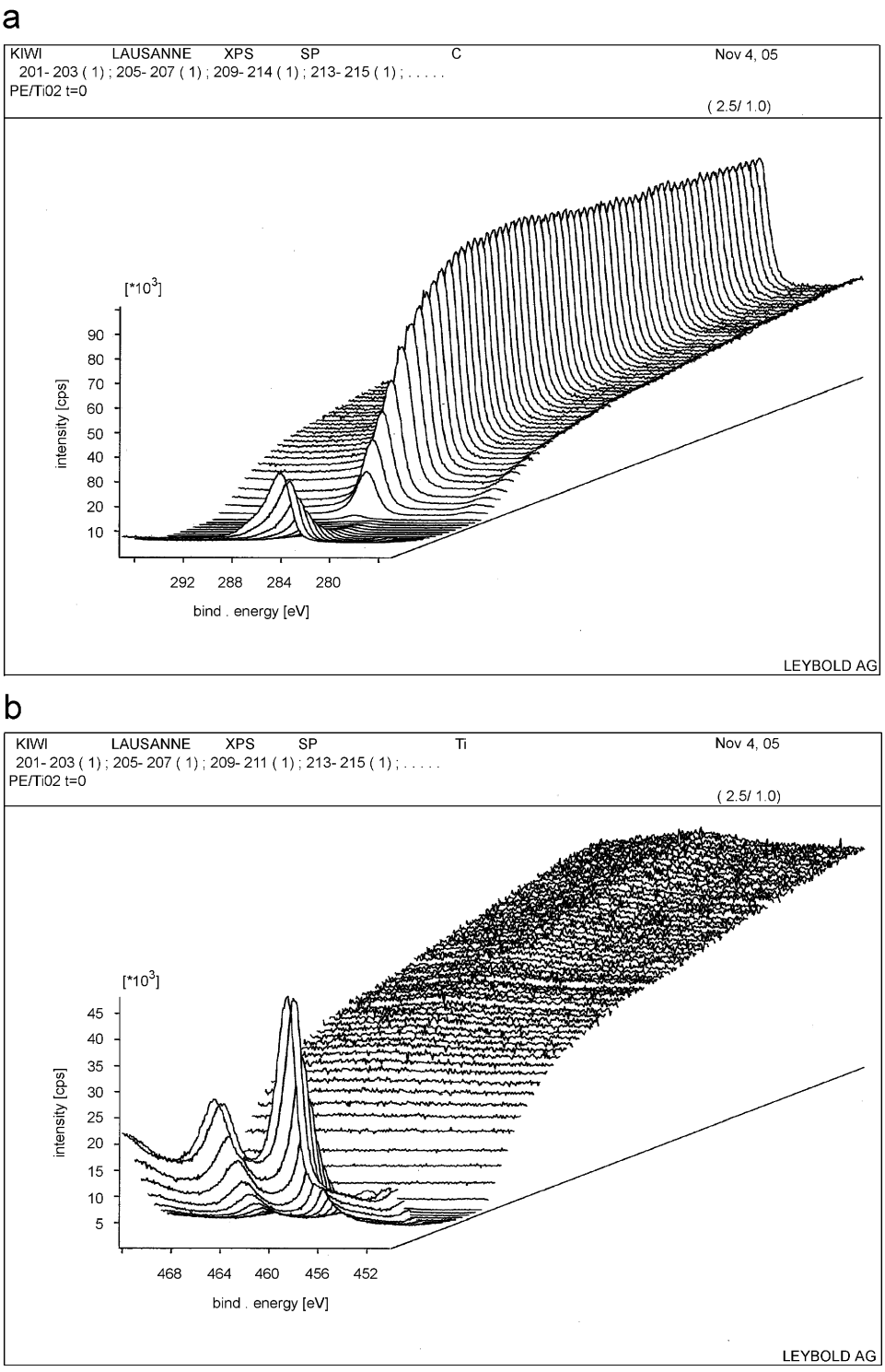

Fig. 10 – (a) Depth profile of an Ar sputtered LDPE-TiO_2 samples showing the C layer distribution. (b) Depth profile of an Ar sputtered LDPE-TiO_2 samples showing the Ti layer distribution. (c) Depth profile of an Ar sputtered LDPE-TiO_2 sample showing the O layer distribution.

decrease from an atomic concentration of 74.58–39.49% (Table 1) when LDPE is loaded with TiO_2. At the beginning of the reaction (only adsorption, time zero) and after 4 h reaction (Fig. 9b) the C-concentration is around 39.08% while at the end of reaction after 10 h Orange II discoloration (Fig. 9c) the C-concentration decreases to 26.77%. Concomitantly, the Ti-concentration increases from values around 14% at times zero and 4 h reaction to almost 19% after 10 h reaction. This clearly indicates that the prepared catalyst is very active and no accumulation of intermediates is observed. Similar conclusion can be drawn from the observed changes in C/Ti intensity ratio. A composite is being produced between Ti– and C– during the

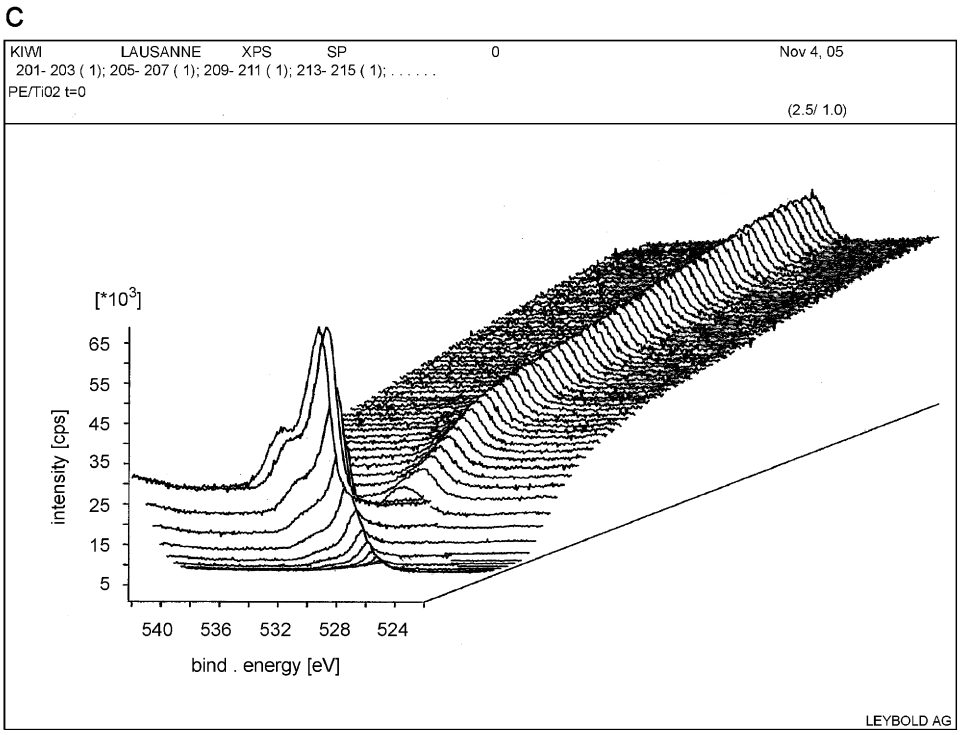

Fig. 10 – (*Continued*)

photocatalysis ensuring the stability of the nanocrystalline TiO_2 on the LDPE film. The evidence for the stability of this composite is accounted for by three experimental observations: (a) the Ti-concentrations reported in Table 1 show that TiO_2 is firmly attached to the LDPE surface and (b) the lack of other peaks than C1 s at 284.6 eV after 10 h reaction indicates that the decomposition of Orange II is efficient and proceeds without accumulation of new C-peaks corresponding to reaction intermediates and (c) The $Ti_2p_{3/2}$ BE shifts between zero and 4 and 10 h (see Table 1). The TiO_2 shows a shift in the $Ti_2p_{3/2}$ line to a lower BE by ~0.3 eV after 4 h and by ~0.45 eV after 10 h reaction indicating a partial reduction of TiO_2. This means the formation of surface species with oxidation state Ti(III) and Ti(IV) involving redox processes during the photocatalysis. The origin of the Ti(III) state may be related to photosensitization by Orange II by the LDPE-TiO_2 film and the formation of an azo-dye radical cation (Vinodgopal and Kamat, 1994) with concomitant charge transfer of the electron to TiO_2e_{cb}- /LDPE or Ti(III) in net sense as shown in Eq. (9)

$$\text{Orange II} + \text{LDPE-TiO}_2 + h\nu \rightarrow [\text{Orange II}^* + \text{LDPE-TiO}_2] \rightarrow \text{Orange II}^{\cdot+} + \text{TiO}_2e_{cb^-}/\text{LDPE}. \quad (6)$$

Fig. 10a shows that the LDPE-TiO_2 after the erosion of the 100 topmost layers due to the sputtering with 5 keV Ar^+-ions. Fig. 10a–c shows the results of XPS depth profile experiments. About 100 layers with thickness of ~2 Å each were eroded for each of the elements investigated. The value of 2 Å for the layer thickness is an approximate value since (a) preferential sputtering effects cannot be excluded (Briggs and Shea, 1990) and (b) the layer thickness for each of the elements investigated depends on its particular sensitivity factor (Shirley, 1972). Fig. 10a shows that the C1s peaks decrease slowly in the 10–15 layers (close to the catalyst surface) due to the TiO_2 loading on the LDPE. A small increase of the C1s peak is noticed in the 5–6 topmost layers may be due to C-impurities on the LDPE-TiO_2 film surface.

Fig. 10b shows that the Ti_2p doublet 8–10 topmost layers increase towards the catalyst surface as expected from the preparation LDPE-TiO_2. Fig. 10c shows the XPS signals of the O1 s doublet at 530.2 and 532.4 eV. O-enrichment was observed after photocatalysis due to the H_2O_2 and other oxidative radicals generated at the surface of the photocatalyst during the abatement of Orange II. In effect an atomic concentration percentage of 47.23% was found after 10 h photo-irradiation vs. 40.80% at time zero as reported in Table 1.

4. Conclusions

This study shows that an effective photodiscoloration of Orange II is possible by LDPE-TiO_2 films using relatively low light intensities and mild oxidative conditions. The LDPE-TiO_2 films have been prepared in an innovative way to allow the optimal photocatalytic performance of the nanocrystalline Degussa TiO_2 P25. No remobilization of the Ti on the LDPE surface was observed and evidence for the Ti–C composite stabilization during the photocatalysis was obtained by XPS data. No surface intermediates were observed during the Orange II photodiscoloration confirming the efficient intervention of the LDPE-TiO_2 films in the photocatalytic process.

Acknowledgment

We wish to thank COST Action 540 PHONASUM "Photocatalytic technologies and novel nanosurface materials, critical issues" for the financial support for this study.

REFERENCES

Bandara, J., Kiwi, J., 1999. Fast kinetic spectroscopy, decoloration and production of H_2O_2 induced by visible light in oxygenated solutions of azo-dye Orange II. New J. Chem. 23, 717–724 (and references therein).

〈blownfilm@reifenhauser.com〉, 1999.

Bozzi, A., Guasaquillo, I., Kiwi, J., 2004. Accelerated removal of cyanides from industrial effluents by supported TiO_2 photocatalysts. Appl. Catal. B 51, 201–209.

Bozzi, A., Yuranova, T., Kiwi, J., 2005. Self-cleaning of wool-polyamide and polyester textiles due to surface TiO_2-rutile modification under daylight irradiation. Photochem. Photobiol. A. 172, 27–34.

Briggs, D., Shea, M., 1990. Auger and X-ray photoelectron spectroscopy. In: Practical Surface Analysis, vol. 1, second ed. Wiley, Chichester, UK.

Dhananjeyan, M., Mielczarski, E., Thampi, K., Buffat, Ph., Bensimon, M., Kulik, A., Mielczarski, J., Kiwi, J., 2001. J. Phys. Chem. B 105, 12046–12055.

Degussa, A.G., 1997. Disperse metal-oxides, 6342. Bäar, Switzerland.

Fernandez, J., Bandara, J., Lopez, A., Buffat, Ph., Kiwi, J., 1999. Photo-assisted Fenton degradation of non-biodegradable azo-dye in Fe-free solutions mediated by cation transfer membranes. Langmuir 15, 185–192.

Kiwi, J., 1986. Quantitative determination of Ti^{3+} formation in semiconductor dispersions induced under light irradiation. J. Phys. Chem. 90, 1493–1496.

Kiwi, J., Grätzel, M., 1987. Specific analysis of surface bound peroxides formed during the photoinduced water cleavage in titanium dioxide based micro-heterogeneous systems. J. Mol. Catal. 39, 63–70.

Mills, A., Lee, S., 1997. An overview of semiconductor photocatalysis. J. Photochem. Photobiol. A 108, 1–35.

Morrison, C., Bandara, J., Kiwi, J., 1996. Sunlight induced decoloration/degradation of non-biodegaradable Orange II dye by advanced oxidation technologies in homogeneous and heterogeneous media. J. Adv. Oxid. Technol 1, 160–169.

Naskar, S., Pillay, S., Chanda, M., 1998. Photocatalytic degradation of organic dyes in aqueous solution with TiO_2 nanoparticles immobilized on foamed polyethylene sheet. J. Photochem. Photobiol. A 113, 257–264.

Oppenlaender, T., 2003. Photochemical Purification of Water and Air. Wiley–VCH Verlag, Weinheim, Germany.

Shirley, A., 1972. High-resolution X-ray photoemission spectrum of the valence of gold. Phys. Rev. 179 (B5), 4709–4716.

Sung, Y., Lee, Y., Lee, M., 2004. Anatase cyrstal growth and photocatalytic characteristics of hot water-treated polyethylene oxide-titania nanohybrids. J. Crystal Growth 267, 312–316.

Vinodgopal, K., Kamat, P.V., 1994. J. Photochem. Photobiol. A 83, 141–148.

Wagner, C., Riggs, W., Davis, I., Moulder, J., Muilenberg, G. (Eds.), 1989. Handbook of X-Ray Photoelectron Spectroscopy. Perkin Elmer Corp., Eden Prairie, MN, 55344, USA.

Yu, J., Zhao, X., Du, J., 2000. Preparation, microstructure and photocatalytic activity of the porous TiO_2 anatase coating by sol–gel processing. J. Sol–Gel Sci. Technol 17, 163–171.